



ELSEVIER

Journal of Alloys and Compounds 239 (1996) 127–130

Journal of
ALLOYS
AND COMPOUNDS

Crystal structure and magnetic behaviour of ternary YbTGa₂ compounds (T = Ni, Pd, Pt) and quaternary solid solutions YbPd_{1-x}Ag_xGa₂

Yu. Grin^{a,1}, K. Hiebl^a, P. Rogl^{a,*}, C. Godart^{b,c}^aInstitut für Physikalische Chemie, Universität Wien, Währingerstraße 42, A-1090 Wien, Austria^bCNRS, UPR209, Pl. A. Briand, F-92195 Meudon, France^cCNRS, LURE-Université de Paris-Sud, F-91405 Orsay, France

Received 24 November 1995

Abstract

Compounds YbTGa₂ with T = Ni, Pd, Pt and alloys YbPd_{1-x}Ag_xGa₂ have been synthesized by argon high frequency melting from metal ingots in tantalum crucibles followed by homogenization annealing at 600 or 400°C respectively. From X-ray powder diffraction data, Yb{Ni,Pd,Pt}Ga₂ was found to be isotypic with MgCuAl₂-type, with a small solid solubility for Ag in YbPdGa₂ (0 ≤ x ≤ 0.2). At 600°C the solid solubility of Pd in βYbAgGa₂ (βYbAgGa₂-type) was 0.7 ≤ x ≤ 1.0. The YbTGa₂ (T = Ni, Pd, Pt) compounds are paramagnets, where the ytterbium adopts the ²F_{7/2} ground state. The magnetic results of the solid solution YbPd_{1-x}Ag_xGa₂ are characterized by an intermediate or mixed valence behavior of the ytterbium atom (Yb²⁺ → Yb³⁺), whereas XAS measurements establish a mixed valence system.

Keywords: Solid solution YbPd_{1-x}Ag_xGa₂; Crystal structure; Magnetism; X-ray absorption spectroscopy; Intermediate valence

1. Introduction

Various structure types have been reported recently for gallides with stoichiometry RETGa₂, where RE is a rare earth metal and T is a transition metal [1–6]. Recently we dealt with the crystal structure of βYbAgGa₂, the structural transition βYbAgGa₂ ⇌ αYbAgGa₂ and the corresponding magnetic transition of practically divalent Yb in βYbAgGa₂ to trivalent Yb in αYbAgGa₂ [7]. In continuation of our systematic interest in ytterbium-containing alloys for their potential to develop valence instabilities or phase transformation-based valence transitions, we focused on ternary Yb alloys with a high density of d-states at the Fermi level.

Thus, the structural behavior and physical properties of compounds YbTGa₂ with T = Ni, Pd, Pt, and particularly the physical behavior in the structurally

closely related solid solutions YbPd_xAg_{1-x}Ga₂ (βYbAgGa₂-type) and YbPd_{1-x}Ag_xGa₂ (MgCuAl₂-type) became the subject of the present investigation.

2. Experimental

Samples with stoichiometry 1:1:2, each with a total mass of about 2.5 g, were prepared from ingots of the elements with a minimum purity of 99.9 mass% by high frequency melting in tantalum crucibles under high purity argon. Weight losses were found to be less than 0.5 mass%. Homogenization heat treatment was performed for 720 h at 600°C. Samples YbPd_{1-x}Ag_xGa₂, x = 0.7, 0.8 and 1.0, were also annealed at 400°C for 720 h to reveal the low temperature modification. After heat treatment the ampoules were quenched in cold water.

For crystallographic characterization, Guinier cameras with monochromated Cu Kα₁ radiation were used. All crystallographic calculations were performed

* Corresponding author.

¹ Present address: Max-Planck-Institut für Festkörperforschung, Heisenbergstraße 1, D-70569 Stuttgart, Germany.

using the crystal structure determination (CSD) program package (vers. 4.10–4.20) [8].

Magnetic measurements for $T > 80$ K were performed in a SUS-10 Faraday-type pendulum magnetometer. In the low temperature region ($T < 100$ K) a SHE-type SQUID magnetometer as well as a Lakeshore a.c. susceptometer were employed.

X-ray absorption measurements were performed at the French synchrotron radiation facility of LURE using the beam delivered by the DCI storage ring, working at 1.85 GeV and around 320 mA on the EXAFS2 station. A double Si (311) crystal was used as a monochromator. Rejection of third order harmonics was achieved by two parallel mirrors adjusted to cut off energies higher than about 11 keV in the incident beam. Experiments were carried out in the range 8860–9040 eV, around the L_{III} edge of Yb, at fixed temperatures (300 K, 10 K). Samples were powdered in cyclohexane to avoid oxidation and filtered through 5 μm nylon tissue. Powder was spread on adhesive Kapton tape and three such tapes were stacked.

3. Results and discussion

3.1. Phase formation and structural chemistry

A detailed investigation of the alloys YbTAgGa_2 , $T = \text{Ni, Pd, Pt, Cu, Au}$, by X-ray powder diffractometry prompted the formation of ternary compounds for $T = \text{Ni, Pd, Pt}$ whose crystal structure appeared different from the βYbAgGa_2 -type. Indexing of the powder diagrams in all cases was successful on the basis of a base centered orthorhombic unit cell of MgCuAl_2 -type, which for $T = \text{Ni, Pd}$ has been described earlier [3,4]. The Pt-containing compound has been characterized for the first time. Interestingly, neither Cu nor Au were observed to form isotypic compounds under the conditions investigated.

With respect to the different valence behavior of the ytterbium atoms in βYbAgGa_2 ($\approx \text{Yb}^{2+}$) and YbPdGa_2 ($\approx \text{Yb}^{3+}$; for details see Section 3.2), a close inspection of the solution behavior along the section $\text{YbPd}_{1-x}\text{Ag}_x\text{Ga}_2$ at 600°C has been performed. Mutual solid solubilities are relatively small, i.e. the maximal solubility for Ag in $\text{YbPd}_{1-x}\text{Ag}_x\text{Ga}_2$ at 600°C is $0 \leq x \leq 0.25$, whereas the homogeneity range for the solubility of Pd in βYbAgGa_2 is restricted to $0.7 \leq x \leq 1$ (see Fig. 1). The crystallographic data for all compounds and alloys of the solid solutions are summarized in Table 1.

A plot of the unit cell dimensions versus x shows a remarkable drop in volume for the replacement of Ag with Pd in βYbAgGa_2 , whereas a corresponding substitution of Pd with Ag in YbPdGa_2 has little effect (see Fig. 1 and Sections 3.2 and 3.3).

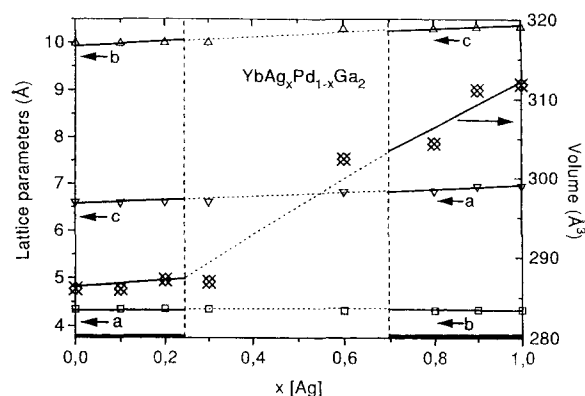


Fig. 1. Unit cell dimensions versus x for the two solid solution range $\text{YbPd}_{1-x}\text{Ag}_x\text{Ga}_2$. The lattice parameters have been interchanged in accordance with the different standard settings of the unit cells. Thick bars at the abscissa denote the homogeneous region.

The rather monotonic change in lattice parameters versus composition reflects the close structural relation of the two structure types, where the Ag-rich solid solution crystallizes as a deformation variant of the MgCuAl_2 -type, which in turn is observed for the Pd-rich counterpart of the solid solution.

3.2. Magnetism

The results of magnetic measurements in the temperature range 5–550 K are summarized in Table 1 and Figs. 2 and 3. For the compounds YbTAgGa_2 with $T = \text{Ni, Pd, Pt}$ the effective magnetic moment μ_{eff} , as derived by a least-squares fit using the general expression $\chi = C(T - \theta_p)^{-1} + \chi_0$, confirmed the ytterbium to adopt the $\text{Yb}^{3+} - ^2F_{7/2}$ ground state configuration (see Fig. 2). Although the values of paramagnetic Curie temperatures θ_p are non-zero, no onset of magnetic ordering has been encountered (see Fig. 2). In the case of the platinum-containing compound, a pronounced deviation of the linear dependence of the $1/\chi$ plot below 100 K is observed. The calculated effective moment in the low temperature region is strongly reduced to a value of $3.3\mu_B$, which is likely due to crystalline field effects.

βYbAgGa_2 , which crystallizes in a unique structure type, proves the ytterbium to be in a non-magnetic ground state [7]. Partial substitution of silver by palladium exhibits a strong influence on the electronic state (possibly a partial overlap of the f-d bands), and hence a magnetic moment is established due to an intermediate valence on the ytterbium site (Fig. 3). Similarly, we observe a reduction of the magnetic moment when palladium is replaced by small amounts ($x \leq 0.2$) of silver (Table 1). Furthermore, in the case of $\text{YbPd}_{0.8}\text{Ag}_{0.2}\text{Ga}_2$ a ferromagnetic ordering of the

Table 1
Crystallographic and magnetic data for alloys YbTGa_2 and $\text{YbPd}_{1-x}\text{Ag}_x\text{Ga}_2$

Composition	Structure type	Space group	a (Å)	b (Å)	c (Å)	V (Å ³)	μ , μ_B	θ_p (K)
YbNiGa_2	MgCuAl_2	$Cmcm$	4.0992(2)	9.8536(5)	6.5950(4)	266.4(1)	4.5	1
YbPdGa_2	MgCuAl_2	$Cmcm$	4.3419(2)	9.9793(4)	6.6014(3)	286.0(1)	4.3	-2
YbPtGa_2	MgCuAl_2	$Cmcm$	4.3027(3)	9.9639(5)	6.6352(5)	284.5(1)	4.4	-22
$\text{YbPd}_{0.9}\text{Ag}_{0.1}\text{Ga}_2$	MgCuAl_2	$Cmcm$	4.3459(4)	9.977(1)	6.5962(6)	286.0(1)	3.5	-17
$\text{YbPd}_{0.8}\text{Ag}_{0.2}\text{Ga}_2$	MgCuAl_2	$Cmcm$	4.3478(3)	9.9923(6)	6.6091(5)	287.1(1)	3.7	-25
$\text{YbPd}_{0.7}\text{Ag}_{0.3}\text{Ga}_2^*$	MgCuAl_2	$Cmcm$	4.3461(2)	9.9899(5)	6.6076(3)	286.9(1)		
$\text{YbPd}_{0.4}\text{Ag}_{0.6}\text{Ga}_2^*$	βYbAgGa_2	$Pnma$	6.8211(7)	4.3106(6)	10.284(1)	302.4(1)		
$\text{YbPd}_{0.2}\text{Ag}_{0.8}\text{Ga}_2$	βYbAgGa_2	$Pnma$	6.8439(5)	4.3214(3)	10.2909(7)	304.3(1)	1.9	-6
$\text{YbPd}_{0.1}\text{Ag}_{0.9}\text{Ga}_2$	βYbAgGa_2	$Pnma$	6.9475(6)	4.3390(4)	10.3206(9)	311.1(1)	0.8	-15
$\beta\text{YbAgGa}_2^{**}$	βYbAgGa_2	$Pnma$	6.9563(3)	4.3362(2)	10.3386(4)	311.85(4)	0.5	7

* Samples multiphase.

** For further details see Ref. [7].

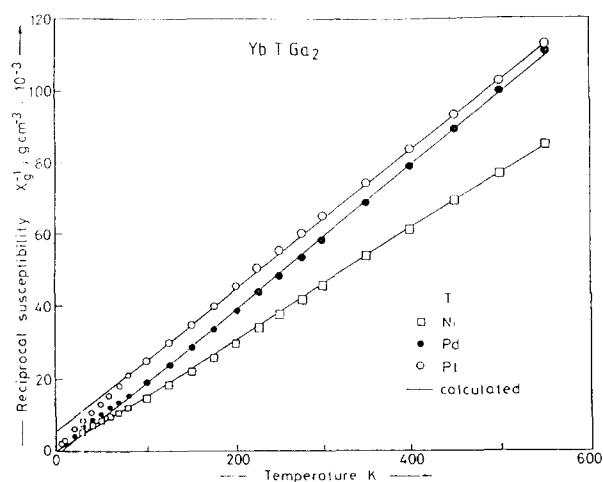


Fig. 2. Reciprocal susceptibilities versus temperature for YbTGa_2 , $T = \text{Ni, Pd, Pt}$.

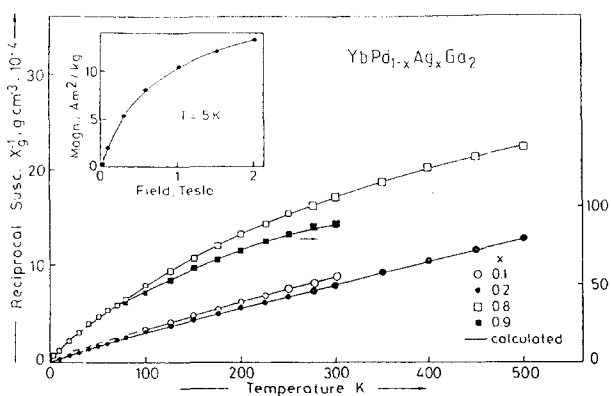


Fig. 3. Reciprocal susceptibilities versus temperature for $\text{YbPd}_{1-x}\text{Ag}_x\text{Ga}_2$. Inset: isothermal magnetization versus magnetic field for $\text{YbPd}_{0.8}\text{Ag}_{0.2}\text{Ga}_2$.

ytterbium sublattice occurs at 5 K, which seems to be related to an increase in unit cell volume as the pure palladium-containing sample remains paramagnetic in

the low temperature regime. According to the isothermal magnetization at $T = 5$ K and an external magnetic field $H = 2$ T, an ordered moment $\mu_s \sim 1\mu_B$ is derived (see inset to Fig. 3). As mentioned in our earlier paper [7], YbAgGa_2 undergoes a structural transition at $T = 440^\circ\text{C}$, which causes a dramatic change of magnetic properties. In the so far unknown low temperature modification YbAgGa_2 , ytterbium atoms bear the full effective moment of the $^2F_{7/2}$ ground state.

3.3. X-ray absorption spectroscopy

L_{III} absorption edge measurements have been performed for $\text{YbAg}_{0.1}\text{Pd}_{0.9}\text{Ga}_2$, $\text{YbAg}_{0.2}\text{Pd}_{0.8}\text{Ga}_2$, $\text{YbAg}_{0.7}\text{Pd}_{0.3}\text{Ga}_2$, $\text{YbAg}_{0.8}\text{Pd}_{0.2}\text{Ga}_2$ and $\text{YbAg}_{0.9}\text{Pd}_{0.1}\text{Ga}_2$ at 10 and 300 K and are summarized in Figs. 4, 5. Fig. 4 shows the L_{III} absorption edge at 10 K for all alloys. The peaks show a double structure, one peak around 8936 eV and a second one around 8943 eV, which corresponds to Yb in a divalent respectively trivalent state. From the change in ratio of

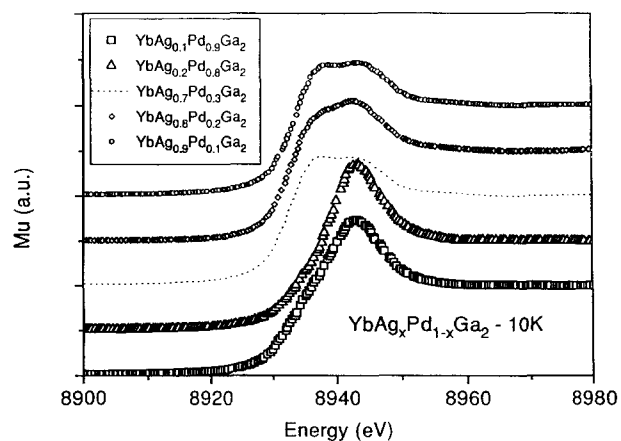


Fig. 4. X-ray absorption spectra at 10 K for $\text{YbAg}_x\text{Pd}_{1-x}\text{Ga}_2$, $x = 0.1, 0.2, 0.7, 0.8$ and 0.9 .

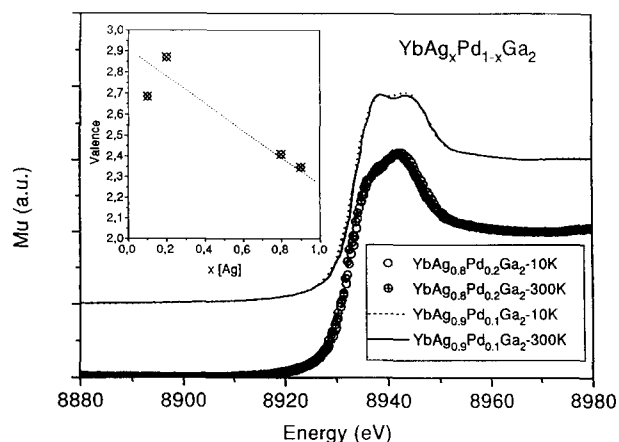


Fig. 5. X-ray absorption spectra for $\text{YbAg}_{0.8}\text{Pd}_{0.2}\text{Ga}_2$ and $\text{YbAg}_{0.9}\text{Pd}_{0.1}\text{Ga}_2$ at 10 and 300 K. The inset shows the valence of Yb versus Ag content in $\text{YbAg}_x\text{Pd}_{1-x}\text{Ga}_2$.

these two peaks with x it clearly appears that the samples on the Pd-rich side are essentially trivalent whereas those on the Ag-rich side are in an intermediate valence state. The curve for $\text{YbAg}_{0.7}\text{Pd}_{0.3}\text{Ga}_2$ corresponds to the α -phase and has been plotted as small circles in Fig. 4. Fig. 5 shows that even in the case of strongly intermediate valence compounds (Ag-rich side) the shapes of L_{III} edge spectra do not change with temperature, an anomalous behavior compared with other Yb-based intermediate valence compounds. Such a temperature independence of the valence in Yb-based samples may occur if the Pd/Ag substitution creates locally two different varieties of Yb coordinations which may then have their own integral valence states. Such a local mixture of two Yb-coordinations is then equivalent to a mixed val-

ence material in which the rare earth atoms are distributed on different crystallographic sites. The usual deconvolution procedure [9] enables us to calculate the values of the valence in the different samples; values at 300 K are plotted as an inset to Fig. 5.

Acknowledgements

This research has been sponsored by the Austrian Fonds FWF under grant P9709, which is gratefully acknowledged. C. Godart is grateful to the Austrian Academic Exchange Service (ÖAD) for financial support (Project 94.44.09).

References

- [1] Yu.N. Grin and Ya.P. Yarmolyuk, *Dopov. Akad. Nauk Ukr. RSR, Ser. A*, 3 (1982) 69.
- [2] O.M. Sichevich, Yu.N. Grin and Ya.P. Yarmolyuk, *Dopov. Akad. Nauk Ukr. RSR, Ser. B*, 7 (1983) 43.
- [3] Ya.P. Yarmolyuk and Yu.N. Grin, *Izv. Akad. Nauk SSSR, Metall.*, 5 (1981) 228.
- [4] Yu.N. Grin, *Dopov. Akad. Nauk Ukr. RSR, Ser. B*, 9 (1984) 33.
- [5] R.E. Gladyshevski, *Thesis*, Lvov, 1987.
- [6] O.M. Sichevich, Yu.N. Grin, I.D. Shcherba, E.E. Terletskaia and M.D. Koterlyn, *Fiz. Met. Metallov.*, 6 (1992) 156.
- [7] Yu.N. Grin, M. Ellner, K. Hiebl, B. Baumgartner and P. Rogl, *J. Alloys Comp.*, 221 (1995) 125–128.
- [8] L.G. Akselrud, Yu.N. Grin, P.Yu. Zavali, V.K. Pecharskii and V.S. Fundamenskii, in *12th Euro. Crystallography Meet., Moscow, Collect. Abstr.*, Vol. 3, 1989, p. 155.
- [9] H. Flandorfer, P. Rogl, K. Hiebl, E. Bauer, A. Lindbaum, E. Gratz, C. Godart, D. Gignoux and D. Schmitt, *Phys. Rev. B*, 50 (1994) 15527.